NATIONAL INSTITUTE FOR FUSION SCIENCE

Dissociative Electron Capture by Halogenated Alkanes and
Kinetics of the Low Energy Electron Attachment by Chloroalkanes

S.A. Pshenichnyuk, N.L. Asfandiarov, W. Barszczewska,
I. Wnorowska, J. Kopyra, I. Szamrej, J. Horáček,
D. Kato and T. Kato

**RESEARCH REPORT
NIFS-DATA Series**

TOKI, JAPAN

Dissociative electron capture by halogenated alkanes and

kinetics of the low energy electron attachment by chloroalkanes

S.A. Pshenichnyuk, N.L. Asfandiarov[1],

Institute of Physics of Molecules and Crystals, October Prospect, 151, Ufa, 450075, Russia

Wiesława Barszczewska, I. Wnorowska, J. Kopyra, I. Szamrej

Chemistry Department, University of Podlasie, Siedlce, Poland

J. Horáček

Faculty of Mathematics and Physics, Institute of Theoretical Physics, Charles

University, Prague, V Holešovičkách 2, 180 00 Praha 8, Czech Republic

D. Kato and T. Kato

National Institute for Fusion Science,

322-6 Oroshi-cho, Toki-shi 509-5292, Japan

ABSTRACT

Data are presented for a series of halogen containing hydrocarbons closely related to the freon molecules studied by the use of electron capture negative ion mass spectrometry. Temperature dependence of negative ion effective yield is discussed. Thermal electron attachment processes in the mixtures of chloroalkanes with carbon dioxide have been investigated using an electron swarm method. All of them (except CH_2Cl_2) attach electrons only in a two-body process. Corresponding rate constants have been determined.

[1] Correspondence author. Institute of Physics of Molecules and Crystals, October Prospect, 151, Ufa, 450075, Russia. Phone/Fax: +7-3472-313538. E-mail: nail@anrb.ru

Introduction

The systematic studies of an interaction of low energy electrons with molecules with further formation of negative ions (NI), both fragmentary and molecular ones, are very important for the understanding of an internal mechanism of many molecular process. Haloalkanes form one of the biggest homologous group where the influence of small systematic changes in chemical structure of the molecule influences their ability to interact with electron. This is probably the largest and most thoroughly investigated group of compounds. So, the study of their negative ion mass spectra will add new results for better understanding how the effectiveness and the mechanism of the electron interaction depend on the structure of the molecule.

A lot of these compounds, freons, play important and very disgraceful role in the atmosphere, not only destroying the ozone layer but also acting as the greenhouse agents. To diminish their negative influence on the environment it is necessary to find methods, which destroy halocarbons existing in the atmosphere. The knowledge of electron interaction processes is of primary importance also for this purpose.

Low energy electron capture by halogenated alkanes has been investigated earlier [1-8]. Low-energy dissociative attachment (DA)

$$e^- + CF_3Cl \rightarrow CF_3Cl^- \rightarrow CF_3 + Cl^-$$

exhibits a temperature effect described well and clearly in the framework of classical theory of DA [2, 9, 10]. For numerical calculation of the temperature effects it is necessary to know a number of parameters of the model: electron affinity (EA) of the molecule and halogen atom, molecular vibrational energies ($\eta\omega$), dissociation energy (DE) and others. The results obtained are in good agreement with the experimental data [2, 5, 9, 10]. The same results may be reached by means of mixed *ab initio*-semiempirical approach of R-matrix theory [6, 11, 12]. It is clear that in the case of dissociative attachment in a low-energy electron-molecular collision the most important point is that of formation of an intermediate negative ion which can dissociate into a fragment ion and appropriate neutral, or lose an additional electron by an autodetachment (AD). Aflatooni and Burrow have found [8] very strong correlation between DA cross sections and appropriate vertical attachment energies for formation of the lowest anion states at the equilibrium geometries of the neutral molecules. This means that the dominant effect in DA cross section must arise from variation in the survival factor of the dissociation anion [8]. An additional information on this parameter may be obtained from the temperature investigations of DA processes.

It is the purpose of this contribution to present our experimental data on dissociative electron attachment to 12ClBr-propane, 13ClBr-propane, 12Cl$_4$Br$_2$-ethane, 112Cl$_3$F$_3$-ethane, 111Cl$_3$F$_3$-ethane, 111F$_2$Cl-ethane, and ClF$_5$-ethane and to study their temperature dependence.

ECNI MS Experiment

ECNI mass spectra of the substances under investigation were measured using a modified [13] MI-1201 mass spectrometer under the following conditions: accelerating voltage 4 kV, electron trap current ~1 μA, FWHM of electron energy distribution $\Delta E_{1/2}$=0.35-0.4 eV, energy of electrons E_{el} varies in the range of 0-10 eV. That type of instrument allows to measure NI curves of effective yield (CEY) as a function of electron energy. Focusing magnet for the electron beam collimating is not shown in Fig. 1. Typical ion source potentials were the following: potential of the anode chamber (#1 in Fig. 1), defined the energy of the electron beam, is varied in the range $-1<U_{el}<+13$ V; the first and the second electron focusing lens (# 4) $-1<U_{1ef}<0$ V, and $0<U_{2ef}<+2$ V respectively; the repel potential (# 7) $-0.8<U_r<-0.2$ V; the ion extraction and the ion focusing lens potentials (# 10) U_{ext}~10±10 V, and U_{if}~±50 V respectively. All tuning potentials are varied in the wide range for the proper adjustment of the ion source. Energy scale refereed using SF_6^-/SF_6.

Tabulated NI mass spectra are presented in Tables 1-7. It is necessary to point out some details in these tables. The column "I_{max}, relative units" means peak maximum of appropriate isotope. With the aim to compare overall (integral) DEA cross section, we present the next column "I^{int}, relative units":

$$I^{int} = \int_{E_{min}}^{E_{max}} I(\varepsilon)d\varepsilon,$$

where E_{min} and E_{max} mean the beginning and the ending energy of the CEY. These values were calculated with taking into account all possible isotopes for each dissociation channel. The next column "Int., %" means the integral intensity of the channel, with taking into account all the isotopes, recalculated to percent contribution into NI mass spectrum.
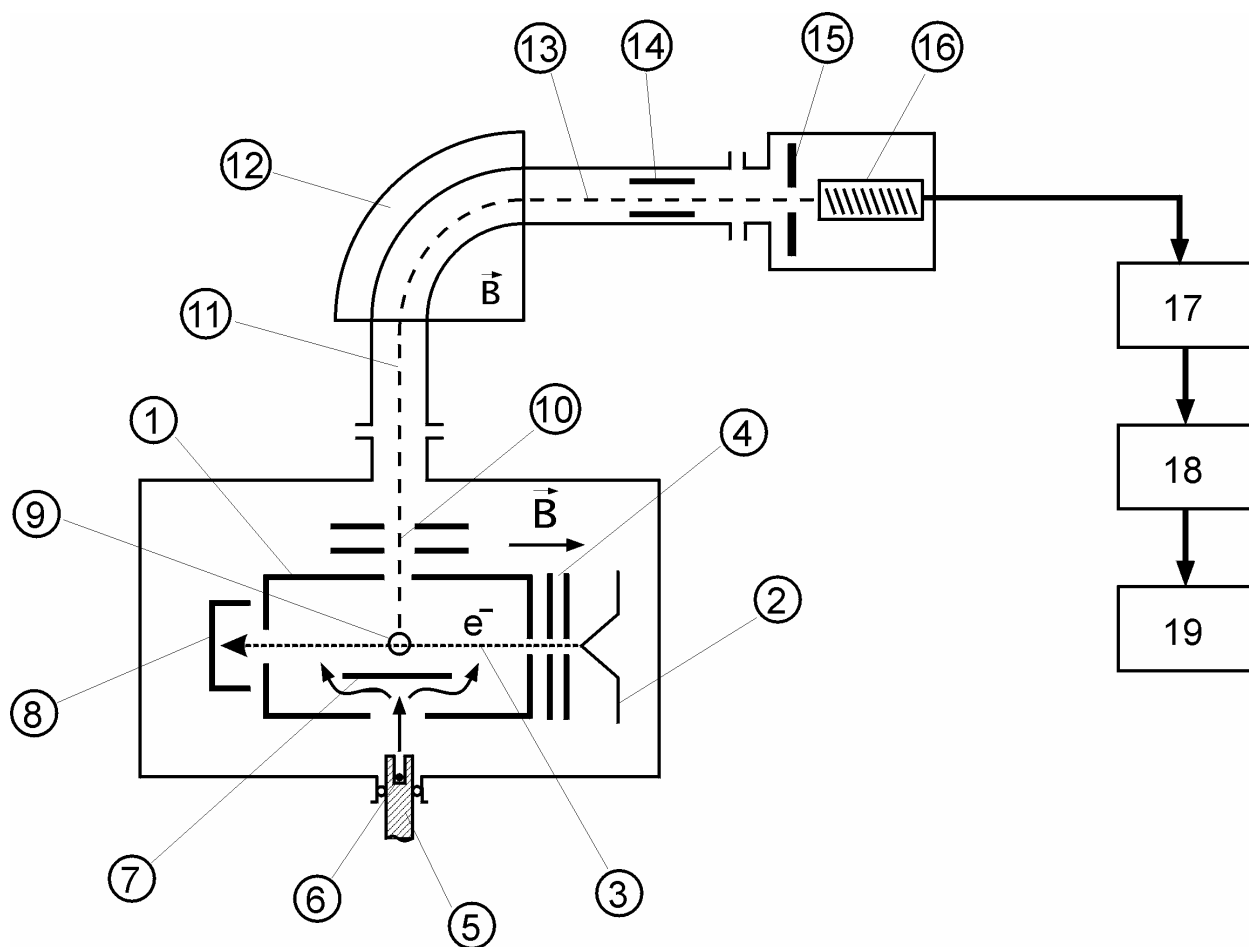
Fig. 1. Schematic view of the ECNI mass spectrometer. Notations: 1. Heating reaction chamber (anode chamber, stainless steel, t=80-300 ^{0}C); 2. Tungsten filament; 3. Electron beam; 4. Electron optics; 5. Heating inflow system (stainless steel rod); 6. Sample under investigation (evaporating); 7. Repel electrode; 8. Electron collector; 9. Interaction region; 10. Ion extraction and focusing lens; 11. First free drift region; 12. Magnet analyzer; 13. Second free drift region; 14. Deflection plates; 15. Ion optics; 16. Secondary electron multiplier; 17. Pulse multiplier; 18. Detection system; 19. Control and record system.

SWARM experimental procedure

The experimental set-up used for the investigations is presented in Figure 2. It consists of an ionization chamber (1) with two parallel electrodes (a) and (b), a Canberra-Packard preamplifier model 2006 (2), a fast (50 ns) oscilloscope with digital memory (3) connected with

a computer and a computer-controlled Canberra-Packard dual 0-5 kV H.V. power supply model 3125 (4).

The electron swarm is produced by an α-particle in the plane of an α-particle source (c). The electron swarm moves to the collecting electrode (a) traversing a distance d (ca. 2 cm) under the influence of a uniform electric field, E, applied between the electrodes. To minimize the influence of the α-source ring it is kept at a zero potential. The drift velocity, W, is a function of the density-reduced electric field, E/N, where N is the total density of the gas in the chamber. In the case of thermal electrons $W = \mu_N \times E/N$, where μ_N denotes the density-normalized electron mobility.

The output pulse from the preamplifier is registered in the digital memory of the oscilloscope. The data are further transferred to the computer memory. The preamplifier converts the input signal from the collecting electrode into an output voltage pulse (whose amplitude is proportional to that of the input signal) with the rise time less than 35 ns. The exponential decay time, t_1, of the pulse is equal to 46 μs (both the values were checked with a step function generator). The electrons traverse the distance d at a time t_0 in the range of 1-50 μs, depending on applied E/N. Thus, we can put that preamplifier follows „immediately" the changes in the electrode potential and discharges both during the pulse and afterwards. It means that the total response function of the preamplifier is that of the decay. To get the shape of the pulse registered by the oscilloscope we have followed the considerations presented in our previous paper [15].

The experiment was performed in such a way that each haloalkane-carbon dioxide mixture was first introduced into the chamber at the highest applied total pressure (ca. 1000 Torr). Always 700 pulses were registered for a given E/N and averaged as described above. The procedure was repeated usually for five E/N values in the rather wide range ($6 \times 10^{-18} - 3 \times 10^{-17}$ V cm^{2}molec.$^{-1}$), where electrons in carbon dioxide are in thermal equilibrium with gas molecules. Next, the mixture was pumped-out to a lower pressure and the measurement procedure was repeated (for ca. 15 consecutive pressures in the range 300-1000 Torr). The whole experiment was carried out for a few different initial concentrations of haloalkane in carbon dioxide.

The one of most important factors in measuring the electron capture rate constants is a purity of an electron acceptor, especially for those with a rather low rate constant value as in the case of monochloro-substituted alkanes because further substitution causes increase in the rate constant by several orders of magnitude and only minute impurities of that kind can cause drastic change in the measured rate constants. The purity of haloalkanes stated by manufacturers is usually no better than 99 % and the nature of impurities is not shown. The usual freeze-pump-thaw technique consists of degassing at liquid nitrogen temperature. This however does not

remove those most dangerous impurities, as they are less volatile. To remove these impurities in each case we prepared a bath with temperature at which the investigated compound has a vapor pressure of a few Torr. It was achieved by choosing a compound with proper melting point and freezing it with liquid nitrogen.

Another important precaution from this point of view is not to measure the rate constants for monosubstituted alkanes immediately after using multi-substituted ones without special care as the last except of having high rate constant sometime absorb strongly. This was also taken into account in our experiment.

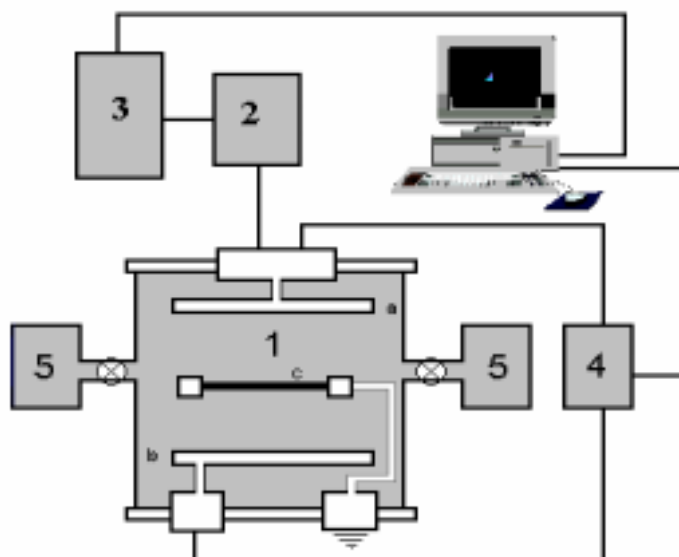All measurements were carried out at room temperature (293 ± 5K).

Figure 2. The experimental set-up used in this investigation (for details see text).

Measured negative ion spectra

12ClBr-propane

Table 1. NI mass spectrum of 12ClBr-propane as a function of the ion source temperature*.

Column 1: mass to charge ratio, column 2: energy of the peak of the DA cross section, column 3: peak intensity in arbitrary units (see the text), column 4: total intensity in arbitrary units, column 5: relative intensity of the given ion including all possible isotopes; column 6: chemical structure of the ion of given m/z.

Ion source temperature 348 K

m/z	E_{max}, eV	I_{max}, relative un.	I^{int}, relative un.	Int., %	Structure
114	0.07	245	28480	1.3	$ClBr^-$
79	0.17	13695	1326295	59.6	Br^-
77	0.07	144	7588	0.3	$(M-Br)^-$
35	0.19	15750	864224	38.8	Cl^-

Ion source temperature 568 K

m/z	E_{max}, eV	I_{max}, relative un.	I^{int}, relative un.	Int., %	Structure
114	0.17	258	34780	2.8	$ClBr^-$
79	0.15	7733	729976	59.0	Br^-
77	0.07	12	626	0.05	$(M-Br)^-$
35	0.15	7793	471068	38.1	Cl^-

Ion source temperature 378 K

m/z	E_{max}, eV	I_{max}, relative un.	I^{int}, relative un.	Int., %	Structure
114	0.11	254	34391	1.4	$ClBr^-$
79	0.19	14055	1393044	58.6	Br^-
77	0.07	109	6449	0.3	$(M-Br)^-$
35	0.18	14790	945338	39.7	Cl^-

* The CEY's for this compound were measured at 348 K, 568 K, and then the temperature of the ion source was decreased again to 378 K with the aim to control of conditions in the ion source. The first (348 K) and the last (378 K) spectra are very similar. It proves correctness of the experiment.

13ClBr-propane

Table 2. **NI mass spectrum of 13ClBr-propane** as a function of the ion source temperature. For details see caption to Table 1.

Ion source temperature 353 K

m/z	E_{max}, eV	I_{max}, relative un.	I^{int}, relative un.	Int., %	Structure
114	0.11	11	2076	0.1	$ClBr^-$
79	0.19	22150	2412725	93.0	Br^-
35	0.17	1458	179536	6.9	Cl^-
	0.75*	1470			

Ion source temperature 563 K

m/z	E_{max}, eV	I_{max}, relative un.	I^{int}, relative un.	Int., %	Structure
114	0.15	19	2320	0.1	$ClBr^-$
79	0.14	45850	4168217	91.3	Br^-
35	0.17	4980	394367	8.6	Cl^-

*   Week resolved peaks.

12Cl$_4$Br$_2$-propane

Table 3. **NI mass spectrum of 12Cl$_4$Br$_2$-ethane as a function of the ion source temperature.** For details see caption to Table 1.

Ion source temperature 348 K

m/z	E_{max}, eV	I_{max}, relative un.	I^{int}, relative un.	Int., %	Structure
162	0.03	2298	77715	4.59	Br_2^-
160	0.04	4789	165065		
158	0.04	2400	82450		
118	0.03	2858	92503		
116	0.05	11760	395138	11.1	$ClBr^-$
114	0.04	8879	299197		
81	0.05	36600	$1.194 \cdot 10^6$		
79	0.05	37050	$1.205 \cdot 10^6$	33.84	Br^-
74	0.09	157	5127		
72	0.1	912	34318	1.28	Cl_2^-
70	0.1	1390	51525		
37	0.1	22250	814700	49.19	Cl^-
35	0.11	72150	$2.672 \cdot 10^6$		

Ion source temperature 438 K

M/z	E_{max}, eV	I_{max}, relative un.	I^{int}, relative un.	Int., %	Structure
162	0.1	450	18769	2.58	Br_2^-
160	0.09	962	37820		
158	0.08	491	20210		
118	0.12	549	21441	6.16	$ClBr^-$
116	0.12	2335	92303		
114	0.11	1797	69780		
81	0.07	8475	331300	22.85	Br^-
79	0.08	9168	348900		

m/z	E_{max}, eV	I_{max}, relative un.	I^{int}, relative un.	Int., %	Structure
74	0.11	55	2020	1.27	Cl_2^-
72	0.15	348	15187		
70	0.13	536	20664		
37	0.13	11318	475040	67.14	Cl^-
35	0.12	37250	$1.524\ 10^6$		

Ion source temperature 533 K

m/z	E_{max}, eV	I_{max}, relative un.	I^{int}, relative un.	Int., %	Structure
162	0.03	126	4237	0.61	Br_2^-
160	0.04	237	7981		
158	0.03	134	4402		
118	0.06	195	6384	1.96	$ClBr^-$
116	0.07	787	26780		
114	0.05	603	20505		
81	0.04	5873	185850	13.79	Br^-
79	0.04	6143	192157		
74	0.1	28	1229		
72	0.08	160	7305	0.73	Cl_2^-
70	0.1	247	11596		
37	0.06	14678	536870	82.91	Cl^-
35	0.06	46150	$1.736\ 10^6$		

Table 4. **NI mass spectrum of 112Cl$_3$F$_3$-ethane.** For details see caption to Table 1.

Ion source temperature 348 K

m/z	E_{max}, eV	I_{max}, relative un.	I^{int}, relative un.	Int., %	Structure
151	0.64	56	2523	0.16	$(M-Cl)^-$
153		36.5	1647		
155		6	269		
70	0.5	157	12324	0.75	Cl_2^-
72			8043		
74			1312		
54	2.15	3.17	229	0.008	ClF^-
56			75		
35	0.29	46650	2901900	98.93	Cl^-
37			946774		
19	2.18	105.75	8686	0.17	F^-

Table 5. **NI mass spectrum of 111Cl$_3$F$_3$-ethane.**

Ion source temperature 348 K

m/z	E$_{max}$, eV	I$_{max}$, relative un.	I^{int}, relative un.	Int., %	Structure
70	0.0	0.35	19.85	0.003	Cl$_2^-$
72			12.95		
74			2.11		
70	6.34	0.18	19.68	0.003	
72			12.84		
74			2.09		
35	0.0	13710	827055	99.83	Cl$^-$
37			269834		
19	6.21	15.55	1820	0.165	F$^-$

Table 6. **NI mass spectrum of 111F$_2$Cl-ethane.** For details see caption to Table 1.

Ion source temperature 348 K

m/z	E$_{max}$, eV	I$_{max}$, relative un.	I^{int}, relative un.	Int., %	Structure
62	11.0	1.1	114	0.08	C$_2$F$_2^-$
55	3.36	1.4	105	0.1	ClHF$^-$
57			34		
54	9.95	0.6	59.6	0.05	ClF$^-$
56			19.4		
45	0.48	1.27	55.5	0.09	C$_2$H$_2$F$^-$
	6.6	0.9	77.2		
	11.35	0.3			
43	8.0	0.4		0.14	C$_2$F$^-$
	10.5	1.6	203		
39	0.0	0.65	40.5	0.07	F$_2$H$^-$
	3.4	0.7	58.6		
	~8	~0.3			
35	0.0	81	-	88.52	Cl$^-$
	1.24	1305	84388		
	3.2	55.5	4957		
	10.4	63	7998		
37	0.0		-		
	1.24		27532		
	3.2		1617		
	10.4		2609		
25	7.04	2.6	-	0.54	C$_2$H$^-$
	8.2	6.7	791		
19	0.07	7	333	10.41	F$^-$
	3.51	141	14848		
	8.4	12.25	-		

Table 7. **NI mass spectrum of ClF$_5$-ethane***

Ion source temperature 348 K

m/z	E_{max}, eV	I_{max}, relative un.	I^{int}, relative un.	Int., %	Structure
135	3.48	4.5	242	0.01	(M-F)$^-$
137		1.5	79		
119	2.76	5.25	261	0.007	(M-Cl)$^-$
35	0.61	16625	1186450	45.37	Cl$^-$
37		5424	387091		
35	2.42	9625	843200	32.24	
37		3140	275102		
19	2.71	8753	776730	22.39	F$^-$

Ion source temperature 473 K

m/z	E_{max}, eV	I_{max}, relative un.	I^{int}, relative un.	Int., %	Structure
135	3.3	4	239	0.011	(M-F)$^-$
137		1.5	78		
119	2.6	3.7	223	0.007	(M-Cl)$^-$
35	0.45	16250	1174330	50.99	Cl$^-$
37		5302	383137		
35	2.3	7700	688175	29.88	
37		2512	224524		
19	2.62	6435	583747	19.11	F$^-$

Ion source temperature 573 K

m/z	E_{max}, eV	I_{max}, relative un.	I^{int}, relative un.	Int., %	Structure
135	0.2	2.6	151	0.007	(M-F)$^-$
137		0.8	50		
135	3.3	3.6	219	0.009	
137		1.2	73		
119	0.56	1.1	89	0.003	(M-Cl)$^-$
119	2.5	3.7	280	0.009	
35	0.39	18025	1247500	55.54	Cl$^-$
37		5881	407009		
35	2.22	6300	573650	25.54	
37		2055	187159		
19	2.53	5978	562800	18.89	F$^-$

* Published previously [14].

SWARM RESULTS

The kinetic results from our swarm experiment together with the available kinetic data are presented in Table 8.

Table 8. Rate constants for the measured chloroalkanes.

Molecule	k ($cm^3 molecule^{-1} s^{-1}$)	$k_{literature\ data}$ ($cm^3 molecule^{-1} s^{-1}$)
CH_2Cl_2	$2{,}6 \cdot 10^{-13}$ *	$4.6 \cdot 10^{-12}$[16], $4.7 \cdot 10^{-12}$[17], $1.5 \cdot 10^{-11}$[18]
CH_3CH_2Cl	$3{,}4 \cdot 10^{-14}$	$<1.6 \cdot 10^{-15}$ [19], $\sim 1 \cdot 10^{-13}$ [20]
CH_2ClCH_2Cl	$2{,}6 \cdot 10^{-11}$	$3.2 \cdot 10^{-11}$ [21]
$CH_2ClCHCl_2$	$1{,}4 \cdot 10^{-10}$	$3.1 \cdot 10^{-10}$ [22,23], $1.8 \cdot 10^{-10}$ [24], $2.1 \cdot 10^{-10}$ [25]
$CHCl_2CHCl_2$	$3{,}2 \cdot 10^{-8}$	
$CH_3CH_2CH_2Cl$	$2{,}7 \cdot 10^{-13}$	
$CH_3CHClCH_3$	$3{,}8 \cdot 10^{-12}$	
$CHCl_2CH_2CH_3$	$5{,}7 \cdot 10^{-11}$	
$CH_3CCl_2CH_3$	$6{,}3 \cdot 10^{-12}$	
$CH_2ClCH_2CH_2Cl$	$1{,}2 \cdot 10^{-11}$	
$CH_2ClCHClCH_3$	$8{,}1 \cdot 10^{-12}$	

* because the rate of this reaction depends on the concentration of CO_2 [26-28] the two-body rate constant has been obtained by the extrapolation to the zero [CO_2].

REFERENCES

1. Illenberger E, Smirnov BM. Uspekhi Fiz. Nauk (Rus.), 1998; **168**: 731-766.

2. Illenberger E, Scheunemann HU, Baumgärtel H. Chem. Phys., 1979; **37**: 21-31.

3. Chutjian A, Alajajian SH. Phys. Rev. A, 1985; **31**: 2885-2892.

4. Christophorou LG (ed) *Electron-molecule interactions and their applications*, Vols. 1, 2 Academic Press, New York 1994.

5. Hahndorf I, Illenberger E, Lehr L, Manz J. Chem. Phys. Lett., 1994; **231**: 460-466.

6. Pearl DM, Burrow PD, Fabrikant II, Gallup GA. J. Chem. Phys., 1995, **102**: 2737-2743.

7. Pearl DM, Burrow PD. J. Chem. Phys. 1994; **101**: 2940-2947.

8. Aflatooni K, Burrow PD, J. Chem. Phys., 2000; **113**: 1455-1464.

9. Lehr L, Miller WH. Chem. Phys. Lett., 1996; **250**: 515-522.

10. Lehr L, Manz J, Miler WH. Chem. Phys., 1997; **214**: 301-312.

11. Wilde RS, Gallup GA, Fabrikant II. J. Phys. B: At. Mol. Opt. Phys., 1999; **32**: 663-673.

12. Fabrikant II, Hotop H. Phys. Rev. A, 2001; 63: 022706-1-022706-10.

13. Khvostenko VI, *Negative Ion Mass Spectrometry in Organic Chemistry*, Moscow, "Nauka", 1981.

14. Asfandiarov NL, Pshenichnyuk SA, Fal'ko VS, Wnoriwska J, Wnoriwski K, Szamrej-Forys I, Nukleonika, 2003; **48**: 83-88.

15. Rosa A, Barszczewska W, Foryś M, Szamrej I, Int. J. Mass Spectrom., 2001; **205**: 85.

16. Sunagawa T, Shimamori H, Int. J. Mass Spectrom. Ion Proc., 1995; **149**: 123.

17. Schultes E, Christodoulides AA, Schindler RN, Chem. Phys., 1975; **8**: 354.

18. Christodoulides AA, Schumacher R, Schindler RN, J. Chem. Phys., 1968; **49**: 1526.

19. Fessenden RW, Bansal KM, J. Chem. Phys., 1970; **53**: 3468.

20. Blaunstein RP, Christophorou LG, J. Chem. Phys., 1968; **49**: 1526.

21. Bansal KM, Fessenden RW, Chem. Phys. Lett., 1972; **15**: 21.

22. Datskos PG, Christophorou LG, Carter JG, Gaseous Dielectrics VI, Plenum Press, New York, 1991; 35.

23. Christophorou LG, Mathis RA, James DR, McCorkle DL, J. Phys. D 1981; **14**: 1889.

24. Smith D, Spanel P, Adv. Atom. Mol. Opt. Phys., 1994; **32**: 307.

25. Smith D, Herd CR, Adams NG, Int. J. Mass Spectrom. Ion Processes, 1989; **93**: 15.

26. McCorkle DL, Christodoulides AA, Christophorou LG, Gaseous Dielectrics IV, Pergamon Press, New York, 1984.

27. Christophorou LG, Zeitschr. Phys. Chem., 1996; **195**: 195.

28. Szamrej I, Tchórzewska W, Kość H, Foryś M, Radiat.Phys.Chem., 1996; **47**: 269.